

Simultaneous and stochastic design of piston-prop TUAV vertical tail and its autonomous system

Erdal Yesilbas

Air Safety Department, Qatar Civil Aviation Authority, Doha, Qatar

Barlas Özgür

Erciyes Project, Turkish Aerospace Industries Inc., Ankara, Turkey

Enes Ozen

Department of Mechanical Engineering, Hasan Kalyoncu University, Sahinbey/Gaziantep, Turkey, and

Tugrul Oktay

Faculty of Aeronautics and Astronautics, Erciyes University, Kayseri, Turkey

Abstract

Purpose – The aim of this paper is to advance autonomous flight performance of a piston-prop tactical unmanned aerial vehicle (TUAV) by simultaneously and stochastically redesigning its vertical tail and autonomous flight control system (AFCS).

Design/methodology/approach – A TUAV is produced in the Erciyes University Unmanned Aerial Vehicle Laboratory. Its vertical tail can be changed before flight. AFCS parameters and vertical tail parameters are simultaneously and stochastically redesigned for maximizing autonomous flight performance index using a stochastic optimization strategy. Obtained results are benefitted during simulation of autonomous flight.

Findings – Applying simultaneous and stochastic design procedure for a piston-prop TUAV owing varying vertical tail and AFCS, autonomous flight performance is maximized.

Research limitations/implications – Permission of Directorate General of Civil Aviation in Republic of Turkey is crucial for flight tests of unmanned air vehicles.

Originality/value – Creating a novel solution for recovering autonomous flight performance of a piston-prop TUAV and also creating a novel algorithm for application of simultaneous and stochastic TUAV's vertical tail and its AFCS design.

Keywords PID controller, TUAVs, Flight control system, Vertical tail, Simultaneous and stochastic design, Performance optimization

Paper type Research paper

1. Introduction

Especially for the past 25 years, unmanned air vehicles (UAVs) have been largely applied in both military and commercial responsibilities because of the reality that they have much superiority with respect to the traditional manned air vehicles. Some of chief superiorities are cheap manufacturing and low operation costs, easily varying configuration according to demands and not endangering the pilot during dangerous missions. UAVs have been applied in civilian tasks such as for aerial photography, agriculture, coast guarding, conservation and customs. They have been also applied in military tasks such as for navy for shadowing enemy fleets, for army for surveillance of enemy activity and for air force for radar system jamming and destruction (please visit, [Austin, 2010](#) for more

UAV applications). In this article, the specific UAV considered is tactical unmanned aerial vehicles (TUAVs). They are heavy UAVs (from 50 to 1,500 kg) and they fly at high altitudes (from 3,000 to 12,000 m). Our TUAV is in the class of close range (CR-TUAV).

For the traditional aerial vehicle design strategy, information for a dynamic model of the any vehicle to be controlled is given to the control engineer who has not any effect on design of this structure. On the other hand, there exists a well-known certainty that the dynamic model design and control model design challenges are not irrelevant (see [Grigoriadis et al., 1996](#) and [Oktay and Sultan, 2013](#) for details on this certainty). Negligible variations in some of the dynamic model variables may improve autonomous flight

The current issue and full text archive of this journal is available on Emerald Insight at: <https://www.emerald.com/insight/1748-8842.htm>



Aircraft Engineering and Aerospace Technology
© Emerald Publishing Limited [ISSN 1748-8842]
[DOI 10.1108/AEAT-11-2024-0311]

This work was supported by Research Fund of The Scientific and Technological Research Council of Turkey (TÜBİTAK) under Project Number: 114M856. This work also has been supported by Erciyes University Scientific Research Projects Coordination Unity under grant number FBA-2024-13808.

Received 4 November 2024

Revised 3 January 2025

Accepted 27 January 2025

performance considerably and remarkably. However, the traditional design strategy does not devote the premium global design. In exclusive strategy, the dynamic vehicle to be controlled and the control model is essential to be simultaneously designed while minimizing a cost function. In this research article, this knowledge is pursued and a piston-prop TUAV constructed in Erciyes University (ERU) and an autonomous flight control system (AFCS) are stochastically and simultaneously designed by considering certain vertical tail variable and AFCS variables while minimizing a cost function capturing some specific autonomous flight trajectory tracking parameters related both longitudinal and lateral flights.

Numerous scientific studies in the relevant literature have been conducted for vertical tail design/redesign to improve different aeronautical performance criteria. For instance, in [Nicolosi et al. \(2013\)](#), a thorough analysis of vertical tail on aerodynamics was performed to evaluate contribution of it to directional stability and control while applying preliminary design stage. A superior approach with respect to the well-known USAF DATCOM and ESDU methods was developed. In [Jing et al. \(2016\)](#), wind tunnel experiments were applied by using an aircraft model having moderate swept wing and a conventional vertical tail. In this work flow, mechanisms responsible for static directional stability were examined. It was obtained from experiments that the vertical tail is the main supplier for static directional stability, whereas the fuselage is the main supplier for static directional instability. In [Larkin and Coates \(2017\)](#), a design analysis of vertical stabilizers on a blended wing body (BWB) aircraft to maintain their appropriateness and effects on stability was researched. It was obtained from this research that a twin-stabilizer design is appropriate for BWB aircraft. In [Bacci and Vagias \(2023\)](#), numerical aerodynamic and radar analyses were applied on three low-radar cross-section airframes, derived from the AVT-183 diamond wing. The geometries were obtained by including dissimilar configurations of vertical stabilizers, to improve lateral and directional characteristics at high angles of attack while minimizing the deterioration of radar signature characteristics. It was found from this study that it is possible to

get adequate lateral/directional characteristics without a substantial deterioration of the radar signature. In [Graboswki \(2023\)](#), the analysis of flying qualities of frequently benefitted unconventional configurations such as canard, flying wing, three surface tandem wing and box wing were applied. The stability analysis was shown in terms of basic static stability and full six DoF dynamic analyses [please visit [Ciliberti et al. \(2017\)](#); [Nicolosi et al. \(2017\)](#); [Carmona and Rejado\(2019\)](#); [Zhou et al. \(2022\)](#); and [Arrieta et al. \(2023\)](#) for vertical tail other design/redesign studies and [Xiong et al. \(2023\)](#) and [Xiong and Li \(2024\)](#) for state of the art UAV AFCS applications].

Here, first of all, effect of vertical tail redesign variable on dynamic models are tried to be explained. After composing dynamic models, brief information for applied TUAV system is given. Then applied autopilot system is briefly mentioned. In addition, applied stochastic optimization approach benefitted for simultaneous and stochastic redesign is also given. Finally, simultaneous and stochastic redesign methodology and also application results are given thoroughly. This paper is the *first research article that* simultaneously and stochastically redesign vertical tail of a piston prop TUAV and its AFCS. Application of a stochastic optimization method that is simultaneous perturbation stochastic approximation (SPSA) for previously mentioned purpose is also one another important contribution of this paper to the literature. This fulfills obtaining the optimal outcomes safe and fast.

2. Effect of vertical tail redesign variable on dynamic models

Here, effect of piston-prop TUAV vertical tail redesign on dynamic models of TUAV is mentioned in short.

[Figure 1](#) shows our piston-prop TUAV manufactured in our drone laboratory and its vertical tail is tried to be redesigned in this article. For any generic fixed-wing TUAV, the longitudinal and lateral state space models are given in [equations 1\(a\)](#) and [\(b\)](#), respectively [please visit also [Nelson, 2007](#): Chapters IV and V; [Etkin and Reid \(1996\)](#): Chapter IV for more details]:

$$\begin{aligned}
 \underbrace{\begin{bmatrix} \dot{x}_l \\ \Delta \dot{u} \\ \Delta \dot{v} \\ \Delta \dot{q} \\ \Delta \dot{\theta} \\ \Delta \dot{h} \end{bmatrix}}_{\dot{x}_l} &= \underbrace{\begin{bmatrix} X_u & X_w & 0 & -g & 0 \\ Z_u & Z_w & u_0 & 0 & 0 \\ M_u + M\dot{w}Z_w & M_w + M\dot{v}Z_w & M_q + M\dot{v}u_0 & 0 & 0 \\ 0 & 0 & 1 & 0 & 0 \\ -\sin(\theta_0) & \cos(\theta_0) & 0 & -u_0\cos(\theta_0) & 0 \end{bmatrix}}_{A_l} \underbrace{\begin{bmatrix} x_l \\ \Delta u \\ \Delta v \\ \Delta q \\ \Delta \theta \\ \Delta h \end{bmatrix}}_{x_l} \\
 &+ \underbrace{\begin{bmatrix} X_T & X_e \\ Z_T & Z_e \\ M_{\delta_T} + M\dot{w}Z_{\delta_T} & M_{\delta_e} + M\dot{v}Z_{\delta_e} \\ 0 & 0 \\ 0 & 0 \end{bmatrix}}_{B_l} \underbrace{\begin{bmatrix} u \\ \Delta \delta_T \\ \Delta \delta_e \end{bmatrix}}_{u} \quad (1a)
 \end{aligned}$$

Figure 1 Photos of our piston-prop TUAV


Source(s): Authors' own work

$$\begin{aligned}
 \begin{bmatrix} \dot{x}_{la} \\ \Delta\dot{\beta} \\ \Delta\dot{p} \\ \Delta\dot{r} \\ \Delta\dot{\phi} \\ \Delta\dot{\psi} \end{bmatrix} &= \overbrace{\begin{bmatrix} \frac{Y_{\beta}}{u_0} & \frac{Y_p}{u_0} & -(1 - \frac{Y_r}{u_0}) & -\frac{g}{u_0} \cos(\theta_0) & 0 \\ L_{\beta}^* + \frac{I_{xz}}{I_{xx}} N_{\beta}^* & L_p^* + \frac{I_{xz}}{I_{xx}} N_p^* & L_r^* + \frac{I_{xz}}{I_{xx}} N_r^* & 0 & 0 \\ N_v^* + \frac{I_{xz}}{I_{zz}} L_v^* & N_p^* + \frac{I_{xz}}{I_{zz}} L_p^* & N_r^* + \frac{I_{xz}}{I_{zz}} L_r^* & 0 & 0 \\ 0 & 1 & 0 & 0 & 0 \\ 0 & 0 & \sec(\theta_0) & 0 & 0 \end{bmatrix}}^{A_{ly}} \begin{bmatrix} x_{la} \\ \Delta\beta \\ \Delta p \\ \Delta r \\ \Delta\phi \\ \Delta\psi \end{bmatrix} \\
 &+ \overbrace{\begin{bmatrix} 0 & \frac{Y_{\delta_r}}{u_0} \\ L_{\delta_a}^* + \frac{I_{xz}}{I_{xx}} N_{\delta_a}^* & L_{\delta_r}^* + \frac{I_{xz}}{I_x} N_{\delta_r}^* \\ N_{\delta_a}^* + \frac{I_{xz}}{I_{zz}} N_{\delta_a}^* & N_{\delta_r}^* + \frac{I_{xz}}{I_{zz}} L_{\delta_r}^* \\ 0 & 0 \\ 0 & 0 \end{bmatrix}}^{B_{la}} \begin{bmatrix} u_{la} \\ \Delta\delta_a \\ \Delta\delta_r \end{bmatrix} \quad (1b)
 \end{aligned}$$

Above, many of the stability derivatives change with respect to the vertical tail redesign parameter. For instance, one of the stability derivative N_{β} changes as following:

$$N_{\beta} = \frac{QSb}{I_{zz}} C_{n_{\beta}}$$

where:

$$\begin{aligned}
 C_{n_{\beta}} &= C_{n_{\beta_{ref}}} + \eta_{vt} V_{vt} C_{L_{vt}} \\
 & * \begin{pmatrix} 0.724 + 3.06 \frac{S_{vt}/S}{1 + \cos\Lambda_{c/4v}} \\ + 0.4 \frac{Z_{ev}}{d} + 0.0009 AR_{vt} \end{pmatrix} \quad (2)
 \end{aligned}$$

Above, $c_{l_{vt}}$ changes with respect to the vertical tail effective aspect ratio, where $AR_e = \frac{1.5 * c_{vt}^2}{S_{vt}} AR$. Determination of $c_{l_{vt}}$ with respect to the AR_e is followed by using the graph in Perkins and Hage (1949: Chapter VIII, p. 324). In this article, S_{vt} and also rudder shape are fixed and only tip and root chord lengths of the vertical tail are varied vice versa. For application of AFCS,

in this article, state space model in equation (1) is required to be controllable or at least stabilizable. It is satisfied in application of this article.

This vertical tail design parameter is symbolized with Λ and illustrated in Figure 2.

In Table 1, definitions of most of symbols benefitted in equations above are introduced.

3. Applied tactical unmanned aerial vehicle system

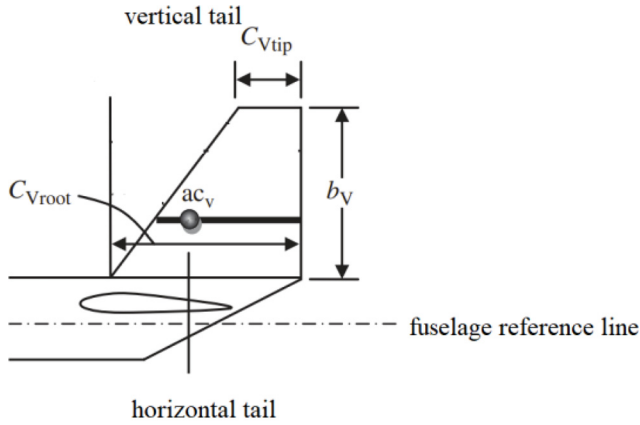
In this section, some of the physical properties of our piston-prop TUAV are summarized.

In Table 2, in the first column, any physical property and in the second column, its magnitude is shared.

4. Applied autopilot system

Here, a PID controller oriented hierarchical autopilot system (HAS) structure is preferred to guide our piston-prop TUAV. Its principal specialties are outlined next: any HAS used for piston-prop TUAV guidance has three layers that are outer, middle and inner ones.

Figure 2 Illustration of vertical tail and design parameter



Source(s): Authors' own work

Table 1 Definition of the symbols for state space modeling

Property	Explanation
X_u, X_w	The contributions of the changes in the velocities u and w with respect to the change of X force
Z_u, Z_w	The contributions of the changes in the velocities u and w with respect to the change of Z force
M_u, M_w	The contributions of the changes in the velocities u and w with respect to the change of M moment
M_q	The contribution of the change in the angular velocity q with respect to the change of M moment
$X_{\delta T}, X_{\delta e}$	The contributions of the changes in the throttle and elevator with respect to the change of X force
$Z_{\delta T}, Z_{\delta e}$	The contributions of the changes in the throttle and elevator with respect to the change of Z force
$M_{\delta T}, M_{\delta e}$	The contributions of the changes in the throttle and elevator with respect to the change of M moment
Y_v	The contribution of the change in the velocity v with respect to the change of Y moment
Y_p, Y_r	The contributions of the changes in the angular velocities with respect p and r to the change of Y force
L_v^*, L_w^*	Starred contributions of the changes in the velocities v and w with respect to the change of L moment
L_p^*, L_r^*	Starred contributions of the changes in the angular velocities p and r with respect to the change of L moment
N_v^*	Starred contribution of the change in the velocity v with respect to the change of N moment
N_p^*, N_r^*	Starred contributions of the changes in the angular velocities p and r with respect to the change of N moment
$Y_{\delta r}$	Starred contribution of the change in the rudder with respect to the change of Y force
$L_{\delta a}^*, N_{\delta a}^*$	Starred contributions of the change in the aileron with respect to the changes of L and N moment
$L_{\delta r}^*, N_{\delta r}^*$	Starred contributions of the change in the rudder with respect to the changes of L and N moment
I_{xz}, I_{zi}, i_{xz}	Inertial terms of the TUAV

Source(s): Authors' own work

Table 2 Physical properties of our piston-prop TUAV

Property	Magnitude
Total mass	50 kg
Maximum payload	15 kg
Wing span	4.0 m
Wing chord length	40 cm
Wing area	1.6 m ²
Aspect ratio of wing	10
Passively morphing property	Yes
Actively morphing property	Yes
Wing taper ratio	Untapered
Powerplant	Liquid fuel powered piston-propeller engine
Engine power	18 HP

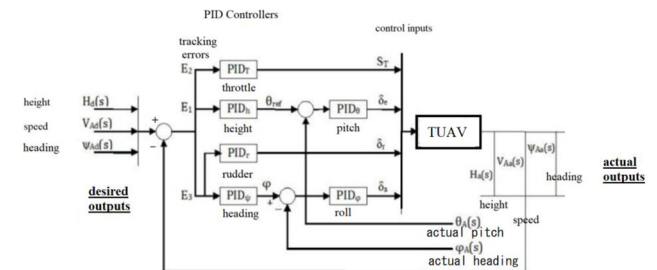
Source(s): Authors' own work

Behaviors of pitch and roll angles are stabilized inside of the inner layer via applying control signals (elevator deflection angle and aileron deflection angle, respectively). Then, heading and altitude are stabilized inside of the middle layer. At the end, tracking x - and y positions of TUAV is succeeded inside of the outer layer. Any HAS has six PID controllers inside (please see Figure 3 for block diagram of any HAS). By using PID blocks, three reference inputs that are altitude, speed and heading angle can be tracked overall (see also Oktay et al., 2016 for details). This commercial autopilot system is chosen in this article as it is the safe and efficient tool for real-time applications and flight tests for such a big and heavy TUAV system.

5. Applied optimization approach for simultaneous and stochastic redesign

Simultaneous and stochastic design of piston-prop TUAV vertical tail and its autonomous system problem to maximize autonomous flight performance is shared next: $\min_{k_{P_{lon}}, k_{I_{lon}}, k_{D_{lon}}, k_{P_{lat}}, k_{I_{lat}}, k_{D_{lat}}, \Lambda} \mathcal{J}$ where $\mathcal{J} = \mathcal{J}_{lon} + a^* \mathcal{J}_{lat}$ (including parameters relevant with not only for longitudinal trajectory tracking but also lateral trajectory tracking) and there exists lower and upper bounds on redesign parameters ($k_{P_{lon}}, k_{I_{lon}}, k_{D_{lon}}, k_{P_{lat}}, k_{I_{lat}}, k_{D_{lat}}, \Lambda$) where these parameters are longitudinal and lateral PID controller gains and vertical tail redesign parameter, respectively. In equation (3), this optimization problem is summarized. Calculation of cost index derivatives according to these design parameters is not analytically achievable. Therefore, definite stochastic

Figure 3 Block diagram of any HAS structure



Source(s): Authors' own work

optimization approaches are crucial. For the solution of this particular redesign problem, a stochastic optimization approach called as SPSA is selected here. It captures much superiority according to the current approaches in the relevant literature. Foremost, it is cheap due to fact that it just benefits two evaluations of the objective for estimating the gradient. Hence, it is much faster than other popular stochastic optimization approaches like genetic algorithms and simulated annealing. In addition, it is practical during solution of constrained optimization problems (see Oktay and Sultan, 2013 for essential points). Here, SPSA is chosen for simultaneous and stochastic piston-prop TUAV vertical tail and AFCS redesign problem. A short definition of SPSA is shared next: Ψ denotes the vector of optimization parameters ($k_{P_{lon}}, k_{I_{lon}}, k_{D_{lon}}, k_{P_{lat}}, k_{I_{lat}}, k_{D_{lat}}, \Lambda$) here and those are six PID controller gains for longitudinal and lateral flights and also one vertical tail redesign parameter. During the application of the classical SPSA, if $\Psi_{[k]}$ is the estimate of Ψ at k -th iteration, then $\Psi_{[k+1]} = \Psi_{[k]} - \Psi_k g_{[k]}$. Here, a_k and d_k are gain sequences, $g_{[k]}$ is the guess of the objective's gradient at $\Psi_{[k]}$ where

$g_{[k]} = \left[\frac{\Gamma_+ - \Gamma_-}{2d_k \Delta_{[k]1}}, \dots, \frac{\Gamma_+ - \Gamma_-}{2d_k \Delta_{[k]p}} \right]^T$, $\Delta_{[k]} \in R^p$ is a vector of p mutually independent mean-zero random variables $\{\Delta_{[k]1}, \dots, \Delta_{[k]p}\}$ filling definite conditions (please visit Sadegh and Spall, 1998; He *et al.*, 2003), Γ_+ and Γ_- are estimates of the objective calculated at $\Psi_{[k]} + d_k \Delta_{[k]}$ and $\Psi_{[k]} - d_k \Delta_{[k]}$, respectively. The adaptation is satisfied by using gain sequences a_k and d_k , which must vary with respect to $a_k = \min \left\{ a / (S + k)^\lambda, 0.95 \min_i \{ \min(\mu_{li}), \min(\mu_{ui}) \} \right\}$ and $d_k = \min \left\{ d / k^\theta, 0.95 \min_i \{ \min(\eta_{li}), \min(\eta_{ui}) \} \right\}$, respectively, where η_l and η_u are vectors whose elements are $(\Psi_{[k]i} - \Psi_{\min_i}) / \Delta_{[k]i}$ for each positive $\Delta_{[k]i}$ and $(\Psi_{\max_i} - \Psi_{[k]i}) / \Delta_{[k]i}$ for each negative $\Delta_{[k]i}$ respectively. Similarly, μ_l and μ_u are vectors whose elements are $(\Psi_{[k]i} - \Psi_{\min_i}) / g_{[k]i}$ for each positive $g_{[k]i}$ and $(\Psi_{[k]i} - \Psi_{\max_i}) / g_{[k]i}$ for each negative $g_{[k]i}$ respectively, and d, a, λ, θ, S are extra SPSA parameters (please see Sadegh and Spall, 1998 for details):

$$\begin{aligned} & 5 \leq k_{P_{lon}} \leq 95, \\ & 0.5 \leq k_{I_{lon}} \leq 9.5, \\ & 5 \leq k_{D_{lon}} \leq 95, \\ & \min_{k_{P_{lon}}, k_{I_{lon}}, k_{D_{lon}}, k_{P_{lat}}, k_{I_{lat}}, k_{D_{lat}}, \Lambda} \mathcal{J} \text{ where } 5 \leq k_{P_{lat}} \leq 95, \mathcal{J} = \mathcal{J}_{lon} + a * \mathcal{J}_{lat}, a = \frac{\mathcal{J}_{lon_0}}{\mathcal{J}_{lat_0}}, \mathcal{J}_{lon} = T_{r_{lon}} + T_{st_{lon}} + M_{p_{lon}}, \mathcal{J}_{lat} = T_{r_{lat}} + T_{st_{lat}} + M_{p_{lat}} \quad (3) \\ & 0.5 \leq k_{I_{lat}} \leq 9.5, \\ & 5 \leq k_{D_{lat}} \leq 95, \\ & 0.9 \leq \Lambda \leq 1.1 \end{aligned}$$

6. Application of simultaneous and stochastic redesign idea

Here, simultaneous and stochastic design of piston-prop TUAV vertical tail and its autonomous system problem is studied. Longitudinal AFCS is required to track 5 degrees of pitch angle and lateral AFCS is required to track 5 degrees of roll angle simultaneously. The cost index captures parameters relevant with not only longitudinal flight but also lateral flight. After application of simultaneous and stochastic redesign approach rather than conventional sequential approach, considerably larger cost index is saved.

In Figure 4, total cost index save (4a), relative cost index save (4b), longitudinal PID gain parameters' changes (4c), lateral PID gain parameters' changes (4d) and root chord length change (4e) are given, respectively. The relative total cost index save according to the default original case ($k_p = 50, k_I = 5, k_D = 50$ for both longitudinal and lateral PID controllers, $\Lambda = 1$ corresponding to original 0.052 m of vertical tail root chord length) is around %49 after application of simultaneous and stochastic redesign idea. In Figure 4, for the initial step of iteration (where design parameters have default values), the number "0" is selected. Furthermore, the final values of design parameters are $k_p = 11.97, k_I = 5.03, k_D = 32.21$ for longitudinal PID controller; $k_p = 40.26, k_I = 1.31, k_D = 49.92$ for lateral PID controller; $\Lambda = 0.9583$ corresponding to final 0.04983 m of vertical tail root chord length.

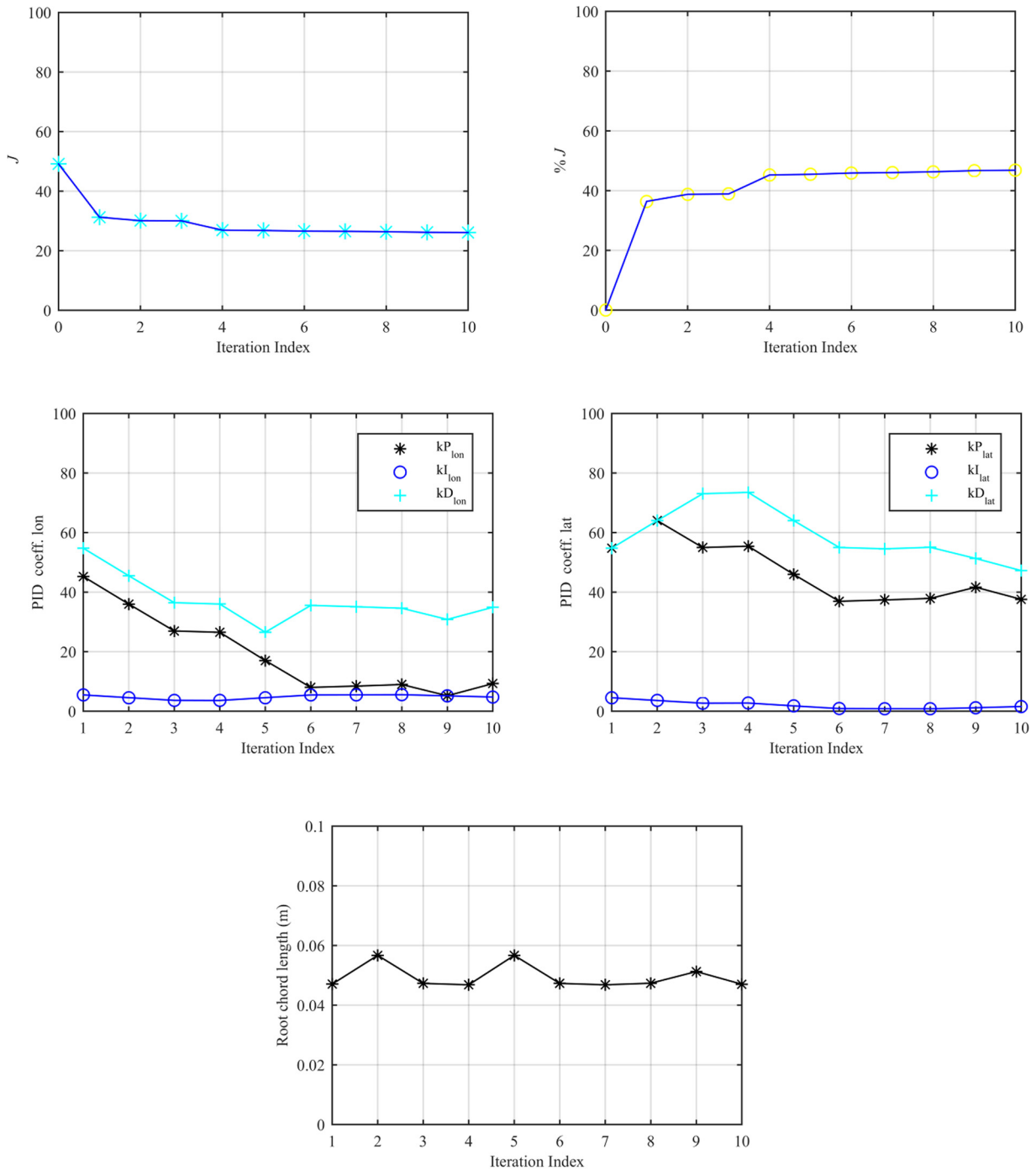
Achievement of our AFCS during existence minor turbulence (Von-Karman turbulence modeling) on the dynamical TUAV system is evaluated as well via benefitting Matlab and Simulink software in simulation environment.

In Figure 5, the closed loop system (CLS) longitudinal responses are given. In Figures 5 and 6, the x -axis denotes time in seconds and y -axis denotes output of interest in degrees. For the symbols inside of these figures, nomenclature at the Appendix can be seen. It can be obviously detected from this figure that our AFCS can successfully track the reference longitudinal trajectory. The components of the cost index (settling time, rise time and overshoot) values are considerably insignificant due to simultaneous and stochastic redesign approach previously mentioned in this article. In addition, other states like longitudinal and vertical velocity states (u and w) that are in secondary interest for longitudinal trajectory tracking do not face to face fast and large oscillations during tracking of longitudinal trajectory. Finally, during existence of bound on control surface (± 30 degrees for elevator here), desired longitudinal trajectory is tracked pleasantly.

Achievement of our AFCS during existence of minor turbulence exists on the lateral dynamical TUAV system is also considered here.

In Figure 6, the CLS lateral responses are presented. It can be evidently seen from this figure that our AFCS can effectively track the reference lateral trajectory. The settling time, rise time and overshoot values for lateral trajectory tracking are also

Figure 4 Optimization results after redesign

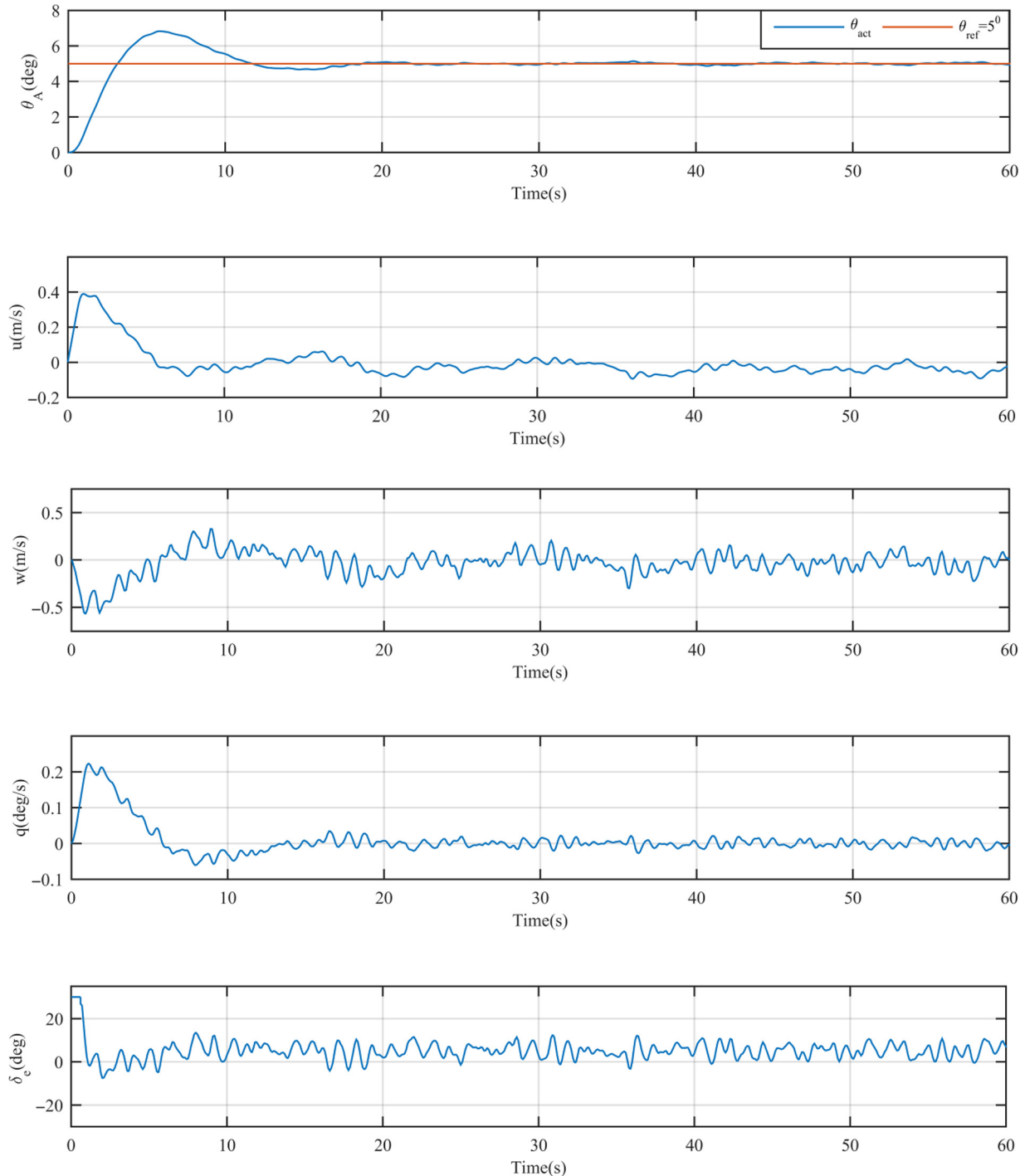


Source(s): Authors' own work

inconsiderable because of the simultaneous and stochastic redesign approach previously mentioned in this article. Besides, the other states (e.g. v and q) that are in secondary interest for lateral trajectory tracking do not face to face fast and large oscillations during tracking of lateral trajectory. At last, during existence of bound on control surface (± 25 degrees for aileron here), desired lateral trajectory is tracked proficiently.

7. Conclusions

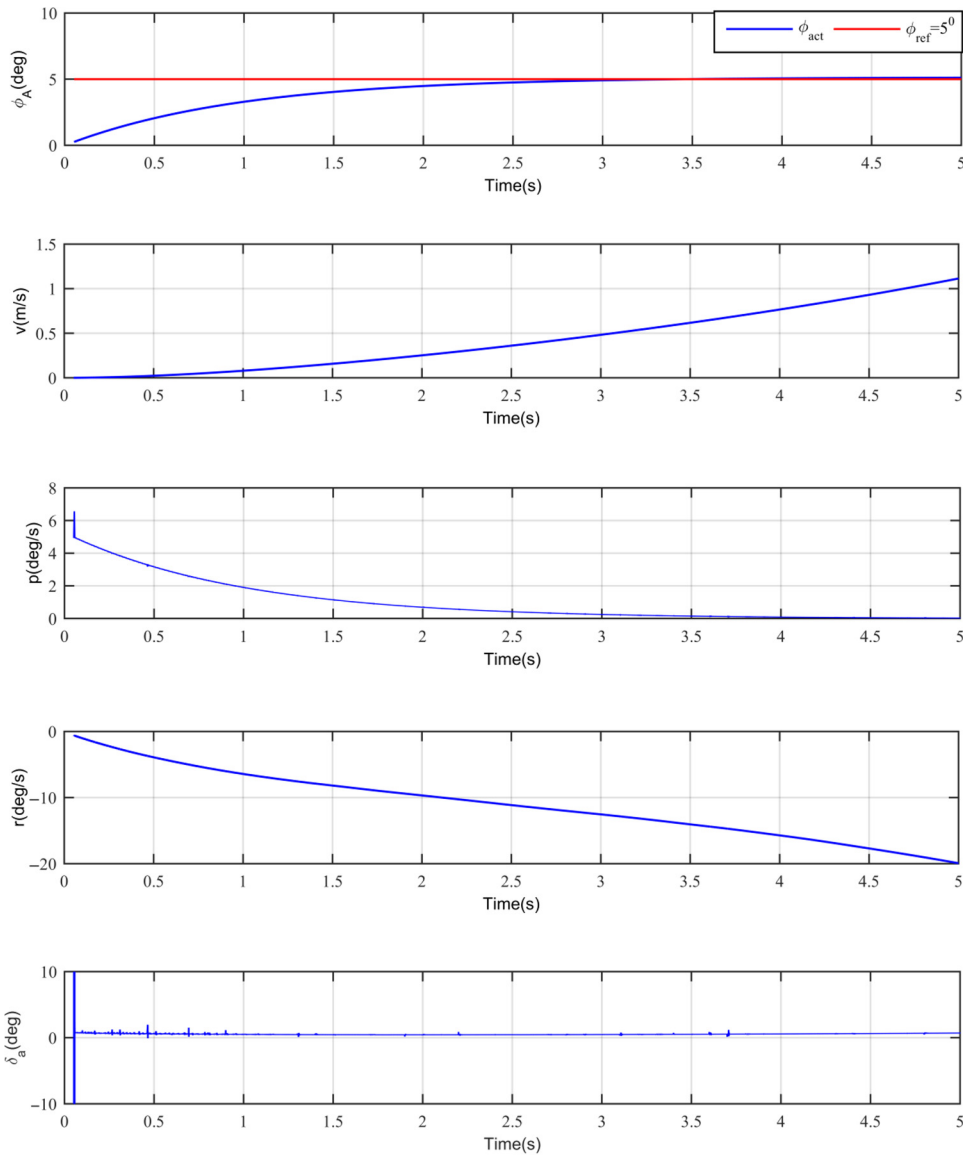
Simultaneous and stochastic redesign of a piston-prop TUAV (tactical unmanned aerial vehicle) vertical tail and its AFCS is investigated for maximizing autonomous flight performance. Data of a TUAV which is produced in our ERU UAV laboratory is benefitted for this research article. Its vertical tail

Figure 5 Longitudinal responses of our piston-prop TUAV

Source(s): Authors' own work

can be varied before flight according to the simultaneous and stochastic design stage results. AFCS design parameters those gains of longitudinal and lateral PID controllers and vertical tail redesign parameter are simultaneously and stochastically redesigned for maximizing autonomous flight performance via benefitting a stochastic optimization strategy named as SPSA. Results obtained are applied for both longitudinal flight and

lateral flight simulations. Important improvement on autonomous flight performance that is almost %49 is reached according to the TUAV which is not redesigned simultaneously and stochastically. That caused less overshoot, settling time and rise time throughout longitudinal and lateral trajectory tracking. Closed-loop responses during existence of pure turbulence in flight period is also investigated and reasonable results that

Figure 6 Lateral responses of our piston-prop TUAV

Source(s): Authors' own work

mean unimportant rise time, settling time and overshoot are obtained. This study contributes piston-prop TUAV operators much more confident, high autonomous performance and peaceful flight opportunity.

References

- Arrieta, O., Campos, D., Rico-Azagra, J., Gil-Martínez, M., Rojas, J. and Vilanova, R. (2023), "Model-based optimization approach for PID control of pitch-roll UAV orientation", *Mathematics*, Vol. 11 No. 15, doi: [10.3390/math11153390](https://doi.org/10.3390/math11153390).
- Austin, R. (2010), *Unmanned Aircraft Systems*, Wiley.
- Bacci, D. and Vagias, I. (2023), "A trade-off analysis between lateral/directional stability and radar cross section requirements of an air-to-air combat airframe", *Aerospace Science and Technology*, Vol. 138, pp. 1-16.
- Carmona, A.S. and Rejado, C.C. (2019), "Vee-tail conceptual design criteria for commercial transport aeroplanes", *Chinese Journal of Aeronautics*, Vol. 32 No. 3, pp. 595-610.
- Ciliberti, D., Vecchia, P.D., Nicolosi, F. and Marco, A. (2017), "Aircraft directional stability and vertical tail design: a review of semi-empirical methods", *Progress in Aerospace Sciences*, Vol. 95, pp. 140-172.
- Etkin, B. and Reid, L.D. (1996), *Dynamics of Flight: Stability and Control*, John Wiley & Sons, New York, NY, chapters, pp. 2-6.
- Grabowski, T.G. (2023), "Flight dynamics of unconventional configurations", *Progress in Aerospace Sciences*, Vol. 137, pp. 1-19.
- Grigoriadis, K.M., Zhu, G. and Skelton, R.E. (1996), "Optimal redesign of linear systems", *Journal of Dynamic Systems, Measurement, and Control*, Vol. 118 No. 3, pp. 598-605.

- He, Y., Fu, M.C. and Marcus, S.I. (2003), "Convergence of simultaneous perturbation stochastic approximation for non-differentiable optimization", *IEEE Transactions on Aerospace and Electronic Systems*, Vol. 48 No. 8, pp. 1459-1463.
- Jing, W., Yankui, W. and Xueying, D. (2016), "An experimental investigation on static directional stability", *Chinese Journal of Aeronautics*, Vol. 29 No. 6, pp. 1527-1540.
- Larkin, G. and Coates, G. (2017), "A design analysis of vertical stabilisers for blended wing body aircraft", *Aerospace Science and Technology*, Vol. 64, pp. 237-252.
- Nelson, R.C. (2007), *Flight Stability and Automatic Control*, 2nd ed. McGraw-Hill, New York, NY, chapters, pp. 2-6.
- Nicolosi, F., Vecchia, P.D. and Ciliberti, D. (2013), "An investigation on vertical tailplane contribution to aircraft sideforce", *Aerospace Science and Technology*, Vol. 28 No. 1, pp. 401-416.
- Nicolosi, F., Ciliberti, D., Vecchia, P.D. and Corcione, S. (2017), "A comprehensive review of vertical tail design", *Aircraft Engineering and Aerospace Technology*, Vol. 89 No. 4, pp. 547-557.
- Oktay, T. and Sultan, C. (2013), "Simultaneous helicopter and control system design", *Journal of Aircraft*, Vol. 50 No. 3, pp. 206-222.
- Oktay, T., Konar, M., Onay, M., Aydin, M. and Abdallah Mohamed, M. (2016), "Simultaneous small UAV and autopilot system design", *Aircraft Engineering and Aerospace Technology*, Vol. 88 No. 6.

- Perkins, C.D. and Hage, R.E. (1949), *Airplane Performance Stability and Control*, Wiley, New York, NY, ISBN 9780471680468.
- Sadegh, P. and Spall, J.C. (1998), "Optimal random perturbations for multivariable stochastic approximation using a simultaneous perturbation gradient approximation", *IEEE Transactions on Automatic Control*, Vol. 43 No. 10, pp. 1480-1484.
- Zhou, L., Pljonkin, A. and Singh, P.K. (2022), "Modeling and PID control of quadrotor UAV based on machine learning", *Journal of Intelligent Systems*, Vol. 31 No. 1, pp. 1112-1122.

Further reading

- Grigoriadis, K.M., Carpenter, M.J., Zhu, G. and Skelton, R.E. (1993), "Optimal redesign of linear systems", *Proceedings of the American Control Conference*, San Francisco, CA.
- Sal, F. (2022), "Simultaneous swept anhedral helicopter blade tip shape and control-system design", *Aircraft Engineering and Aerospace Technology*, doi: [10.1108/AEAT-02-2022-0050](https://doi.org/10.1108/AEAT-02-2022-0050).
- Xiang, J.J. and Li, C. (2024), "Neuroadaptive sliding mode tracking control for an uncertain TQUAV with unknown controllers", *International Journal of Robust and Nonlinear Control*, Vol. 35 No. 2, pp. 579-590.
- Xiang, J.J., Guo, N.H., Mao, J. and Wang, H.D. (2022), "Self-tuning sliding mode control for an uncertain coaxial octorotor UAV", *IEEE Transactions on Systems, Man, and Cybernetics: Systems*, Vol. 53 No. 2, pp. 1160-1171.

Appendix

Nomenclature

p, q, r	= Piston-prop TUAV angular velocities (i.e. longitudinal lateral, vertical, respectively) [deg/s];
u, v, w	= Piston-prop TUAV linear velocities (i.e. longitudinal lateral, vertical, respectively) [m/s];
ϕ_A, θ_A, ψ_A	= Piston-prop TUAV Euler angles (i.e. longitudinal lateral, vertical, respectively) [deg];
$\delta_T, \delta_\omega, \delta_\alpha, \delta_r$	= Throttle control, longitudinal control-elevator, lateral control-aileron and lateral control-rudder [deg];
h	= Piston-prop TUAV altitude [m];

J	= Controller cost or cost index [];
V	= Sensor noise intensity;
W	= Process noise intensity; and
T_r, T_{st}, M_p	= Rise time, settling time, overshoot.

Abbreviations

AR	= Aspect ratio of wing;
AFCS	= Autonomous flight control system;
HAS	= Hierarchical autopilot system;
SPSA	= Simultaneous perturbation stochastic approximation;
UAV	= Unmanned aerial vehicle; and
TUAV	= Tactical unmanned aerial vehicle.

Corresponding author

Enes Ozen can be contacted at: enes.ozen@hku.edu.tr